

BELLCOMM, INC.

955 L'ENFANT PLAZA NORTH, S.W., WASHINGTON, D.C. 20024

COVER SHEET FOR TECHNICAL MEMORANDUM

TITLE- Analysis of a Test Method for
Measuring Resonant Frequencies of
Loaded Hydraulic Feed Lines

FILING CASE NO(S)-

320

TM-70-1033-1

DATE- January 23, 1970

AUTHOR(S)- G. C. Reis

FILING SUBJECT(S)

(ASSIGNED BY AUTHOR(S))-

POGO, Saturn V Testing
Electrical-Fluid Analogy
Mathematical Model
Fluid Line Analysis

ABSTRACT

This memorandum analyzes the MSFC facility for testing the resonant frequencies of fluid feed lines. A theoretical analysis of a simple model of the test facility is presented. This is followed by derivation of equations for a more complete model for computer simulation. The computer results, theoretical results and test results are in good agreement.

**CASE FILE
COPY**

DISTRIBUTION

COMPLETE MEMORANDUM TO

CORRESPONDENCE FILES:

OFFICIAL FILE COPY
plus one white copy for each
additional case referenced

TECHNICAL LIBRARY (4)

NASA Headquarters

T. A. Keegan/MA-2
C. H. King, Jr./MAT
W. E. Stoney/MA
R. L. Wetherington/MAT-4

MSFC

L. A. Gross/S&E-ASTN-PAA
L. B. Mulloy/S&E-ASTN-A
J. B. Sterett, Jr./S&E-ASTN-A
A. L. Worlund/S&E-ASTN-PTF
J. Blackstone/S&E-CSE-1

NR - Space Division

W. Ezell
L. Kraft

NR - Rocketdyne

J. Fenwick
E. Larson

Bellcomm, Inc.

G. M. Anderson
A. P. Boysen, Jr.
D. R. Hagner
H. A. Helm
J. J. Hibbert
B. T. Howard
D. B. James
R. K. McFarland
J. Z. Menard
L. D. Nelson
J. J. O'Connor
I. M. Ross
J. A. Saxton
P. F. Sennewald
R. V. Sperry
J. W. Timko
R. L. Wagner
M. P. Wilson

All Members of Department 1033
All Members of Department 2031
Department 1024 File

SUBJECT: Analysis of a Test Method for
Measuring Resonant Frequencies of
Loaded Hydraulic Feed Lines - Case 320

DATE: January 23, 1970

FROM: G. C. Reis

TM-70-1033-1

TECHNICAL MEMORANDUM

INTRODUCTION

Important parameters in POGO studies are the resonant frequencies of the various fluid feed lines (inboard and outboard fuel and lox). To determine these frequencies, a test facility was constructed at MSFC and various tests were run. It was generally felt that the frequency thus determined by the first such test was too low. Certain changes were made in the test facility and the test rerun. This time the frequency was much higher.

This fact caused concern for many people ("What will the frequency be next week?"). Some questions were raised about the validity of determining the frequencies by measuring ratios of dependent pressures when flow was the independent variable. The test results contained the unexplained anomaly that different pressures peaked at different frequencies.

In the face of these uncertainties, MSFC personnel indicated that it would be helpful if Bellcomm would analyze the test facility and procedures with the aim of answering the various questions. This memorandum presents the results of a theoretical study and a computer analysis of the test method.

DESCRIPTION OF TEST FACILITY AND PROCEDURES

Figure 1 is a simplified diagram of the test facility. The location of pressure transducers in the system are indicated by dots. The input signal is provided by a variable-orifice located in the pulser line. Changing this orifice varies the amount of fluid bypassing the pump and thus causes flow perturbations in the line. This configuration represents the second test. For the first test, the accumulator was absent and the pulser line pressure transducer was closer to the line under test.

The data of interest are the pressures indicated by the transducers located at the pump, at the sump, and along the pulser line. The data processing consists of first converting

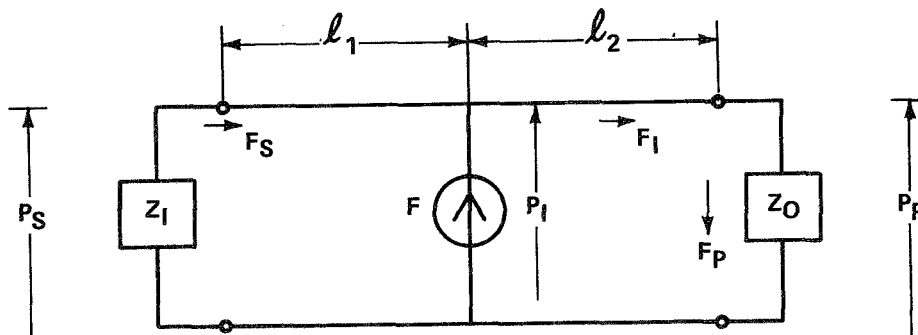
the pressure signals to digital form and then computer construction of power spectral densities (PSD). The ratio of cross-spectral density to autospectral density yields the transfer functions by well-known results in statistical signal analysis. Since the data processing follows standard techniques, it is assumed that the resulting PSD's are an accurate representation of the frequency characteristics of the signals.

OUTLINE OF THE ANALYSIS

The test facility was analyzed on two levels. First a simplified mathematical model, amenable to theoretical analysis, was considered. This model was analyzed with a view towards answering some of the questions posed previously. On the basis of this study certain conclusions were drawn. Then a more complicated model of the test facility was subjected to computer analysis to verify and improve the accuracy of the theoretical conclusions. On the basis of these two studies conclusions were made concerning the accuracy of the test facility and recommendations made for improving future tests. The answers to the various questions on the test results were provided by the analysis.

THEORETICAL ANALYSIS

Let P, F represent pressure and flow, respectively. Let the subscripts S, P, I stand for sump, pump and input, respectively. The simplified model for theoretical study assumes that the entire test facility above the sump pressure transducer and the entire test facility below the pump transducer can be represented as fluid impedances. (It is not required that they be rational functions of frequency.) If the impedance at the driving end of the line is called Z_I and the terminating impedance is called Z_O , then the simplified model consists of a fluid line terminated at one end by Z_I , at the other end by Z_O , and driven by a flow source F somewhere in the line. An electrical network equivalent of this configuration is shown below. Here the total length of the line under test is $l = l_1 + l_2$.



The mathematical model chosen for a steady-state sinusoidal analysis of the fluid line is the steady state distributed parameter model. Assuming the input flow to be unity, the following matrix equation describes the model.

$$\begin{bmatrix} -C_1 & jZ_C S_1 & 1 & 0 & 0 & 0 \\ jS_1/Z_C & -C_1 & 0 & 1 & 0 & 0 \\ 0 & 0 & -C_2 & jZ_C S_2 & 1 & 0 \\ 0 & 0 & jS_2/Z_C & -C_2 & 0 & 1 \\ 1 & Z_I & 0 & 0 & 0 & 0 \\ 0 & 0 & 0 & 0 & 1 & -Z_0 \end{bmatrix} \begin{bmatrix} P_S \\ F_S \\ P_I \\ F_I \\ P_P \\ F_P \end{bmatrix} = \begin{bmatrix} 0 \\ 1 \\ 0 \\ 0 \\ 0 \\ 0 \end{bmatrix} \quad (1)$$

where

$$C_i = \cos \frac{\omega l_i}{a} \quad Z_C = a/gA$$

$$S_i = \sin \frac{\omega l_i}{a} \quad a = \text{wave speed in line}$$

$$A = \text{area of line}$$

The determinant of this system can be calculated to be

$$-(\alpha Z_0 + \beta) \quad (2)$$

where

$$\alpha = C_2(C_1 + j \frac{Z_I}{Z_C} S_1) + \frac{jS_2}{Z_C} (Z_I C_1 + jZ_C S_1)$$

$$\beta = jZ_C S_2(C_1 + \frac{Z_I}{Z_C} S_1) + C_2(Z_I C_1 + jZ_C S_1)$$

Determination of Resonant Frequencies

Since the resonant frequencies of this system are zeros of the determinant we require that

$$\beta = -\alpha Z_0$$

This can be eventually simplified to

$$\tan \frac{\omega l_2}{a} = \frac{jc - b \tan \omega l_1/a}{b + jc \tan \omega l_1/a} \quad (3)$$

where

$$c = Z_I + Z_0$$

$$b = Z_C + \frac{Z_0 Z_I}{Z_C}$$

However, by the well-known formula for tangent of sums of angles, this condition is equivalent to

$$\tan \frac{\omega (l_1 + l_2)}{a} = j \frac{c}{b} \quad (4)$$

or

$$\tan \frac{\omega l}{a} = j \frac{Z_I + Z_0}{Z_C \left[1 + \frac{Z_0 Z_I}{Z_C} \right]}$$

It is well known* that the resonant frequencies of a line of length ℓ , terminated in Z_0' are given by

$$\tan \frac{\omega \ell}{a} = j \frac{Z_0'}{Z_C}$$

If Z_0' is the load which the line will have in actual operation, then the natural resonant frequencies of the test set-up will agree with the natural frequencies of the line (with load) exactly when

$$Z_0' = \frac{Z_I + Z_0}{1 + \frac{Z_0 Z_I}{Z_C^2}} \quad (5)$$

If Z_0 equals Z_0' (as is usually the case) then the test set-up gives perfect results only when $Z_0 = Z_C$ or $Z_I = 0$.

Determination of Pressure Zeros

The zeros of P_S are the zeros of the cofactor of the element in the second row, first column of the system matrix. It is easy to calculate the pertinent equation as

$$Z_I (Z_0 C_2 + j Z_C S_2) = 0 \quad (6)$$

Hence the zeros of P_S are either zeros of Z_I or satisfy

$$\tan \frac{\omega \ell_2}{a} = j \frac{Z_0}{Z_C} \quad (7)$$

*E. W. Kimbark, "Electrical Transmission of Power and Signals", Wiley and Sons, 1949, p. 102.

The zeros of P_I are zeros of the cofactor of the element in the second row, third column of the matrix. The equation can be calculated to be

$$(C_1 Z_I + j Z_C S_1) (Z_O C_2 + j Z_C S_2) = 0 \quad (8)$$

Hence the zeros of P_I satisfy either of the following equations

$$\tan \frac{\omega l_1}{a} = j \frac{Z_I}{Z_C} \quad (9)$$

$$\tan \frac{\omega l_2}{a} = j \frac{Z_O}{Z_C} \quad (10)$$

The zeros of P_P are zeros of the cofactor of the element in the second row, fifth column. The equation is

$$Z_O (Z_I C_1 + j Z_C S_1) = 0 \quad (11)$$

Hence zeros of P_P are either zeros of Z_O or satisfy the equation

$$\tan \frac{\omega l_1}{a} = j Z_I / Z_C \quad (12)$$

The next pressure zero of interest is that of the pulser line transducer. Let this pressure be P_O and assume that the fluid line between this transducer and the test line can be represented as a simple inertance L_P . If Z_1 is the impedance "seen" by P_I looking toward Z_I and Z_2 is the impedance "seen" by P_I looking toward Z_O , then P_O is zero whenever the impedance "seen" by P_O is zero, that is

$$j\omega L_P + \frac{Z_1 Z_2}{Z_1 + Z_2} = 0 \quad (13)$$

where

$$Z_1 = Z_C \frac{Z_I + jZ_C \tan \omega \ell_1 / a}{Z_C + jZ_I \tan \omega \ell_1 / a} \quad (14)$$

$$Z_2 = Z_C \frac{Z_O + jZ_C \tan \omega \ell_2 / a}{Z_C + jZ_O \tan \omega \ell_2 / a} \quad (15)$$

(Expressions (14) and (15) follow from the derivation in Appendix A.) The solution of (13), even under reasonable simplifying assumptions, is analytically intractable. Since all ratios in test results involve P_0 in the denominator, and since the maximum of such ratios can be reasonably expect to occur near the minimum of P_0 and since this maximum is assumed to be the resonant frequency of the system, it is important to reach conclusions about the zeros of P_0 (i.e., solutions of equation (13)). Therefore we will consider certain special cases.

Certain Special Cases

As the impeller blades of the pump rotate, a foam is created at the pump inlet. This foam has the characteristics of a cavitation compliance. The parameter used in most POGO models is the resonant frequency of the line, terminated in this cavitation compliance. If we let ω_L be this frequency, and let the cavitation compliance be C_B (yielding an impedance $Z_0 = 1/j\omega C_B$) then equation (4) (with $Z_I = 0$) yields

$$\tan \frac{\omega_L \ell}{a} = \frac{1}{\omega_L Z_C C_B} \quad (16)$$

In addition assume that Z_I of the test facility is essentially an inertance L_I (i.e., $Z_I = j\omega L_I$). Let ω_S be the resonant frequency of the test facility under this assumption. Then equation (4) yields

$$\tan \frac{\omega_S \ell}{a} = \frac{\frac{1}{\omega_S C_B} - \omega_S L_I}{Z_C \left[1 + \frac{L_I / C_B}{Z_C^2} \right]} \quad (17)$$

It should be clear that $\omega_S < \omega_L$ for $L_I > 0$. (In fact, rough hand calculations indicate that $\omega_S \approx 0.9 \omega_L$. On this basis alone the test facility would yield results 10% too small.)

Using the same two assumptions for Z_I and Z_O in equations (14) and (15) yields

$$Z_1 = jZ_C \frac{\frac{\omega L_I}{Z_C} + \tan \omega \ell_1 / a}{1 - \frac{\omega L_I}{Z_C} \tan \omega \ell_1 / a} \quad (18)$$

$$Z_2 = -jZ_C \frac{\frac{1}{\omega C_B Z_C} - \tan \omega \ell_2 / a}{1 + \frac{1}{\omega C_B Z_C} \tan \omega \ell_2 / a} \quad (19)$$

Since we are attempting to solve (13), we are interested in the behavior of $Z_1 Z_2 / (Z_1 + Z_2)$. Note that $Z_1 Z_2$ is purely real, and $Z_1 + Z_2$ is purely imaginary. Thus $Z_1 Z_2 / (Z_1 + Z_2)$ is purely imaginary.

Hence (13) can be written

$$\omega L_P + \frac{Z_1 Z_2}{j(Z_1 + Z_2)} = 0 \quad (20)$$

If (18) and (19) are substituted into (20) and then solved for ω , we will have solutions to (13) (i.e., the zeros of P_0). However this is too complicated for hand calculation. We shall therefore be satisfied to show that for $\omega = \omega_L$ (solution of (16)) there is a value of L_P which satisfies (20). In other words we will show that there exists some L_P which results in a zero of P_0 at ω_L .

Equation (19) evaluated at $\omega = \omega_L$ yields

$$\begin{aligned} jZ_2 &= Z_C \frac{\tan \omega_L \ell_1 / a - \tan \omega_L \ell_2 / a}{1 + \tan \omega_L \ell_1 / a \tan \omega_L \ell_2 / a} \\ &= Z_C \tan \omega_L (\ell_1 - \ell_2) / a \\ &= Z_C \tan \omega_L \ell_1 / a \end{aligned} \quad (21)$$

Equation (18) evaluated at $\omega = \omega_L$ yields

$$jZ_1 = - \frac{\omega_L L_I / Z_C + \tan \omega_L \ell_1 / a}{1 - \omega_L L_I / Z_C \tan \omega_L \ell_1 / a} \quad (22)$$

Substituting (21) and (22) into (20) and solving for L_P :

$$L_P = \frac{Z_C \tan \omega_L \ell_1 / a [\omega_L L_I / Z_C + \tan \omega_L \ell_1 / a]}{\omega_L \omega_L L_I / Z_C [1 + (\tan \omega_L \ell_1 / a)^2]} \quad (23)$$

This always results in $L_P > 0$ since $\omega_L \ell / a < \pi/2$ (from (16)) and $\omega_{L1} \ell_1 / a < \omega_L \ell / a$. To get an estimate of the magnitude of L_P assume $\tan \omega_L \ell_1 / a$ is nearly equal to $\omega_L \ell_1 / a$ and let $Z_C \ell_1 / a = L_1$ (the inductance of the line between Z_I and the pulser). Then

$$L_P = \frac{L_1 (L_I + L_1)}{L_I (1 + (\omega_L \ell_1 / a)^2)} \quad (24)$$

As a working "rule of thumb", let $L_I \ll L_1$ and assume high wave speed ($\omega_L \ell_1 \ll a$). Then (24) becomes

$$L_P = L_1^2 / L_I \quad (25)$$

Hence there is some critical value of L_P which yields zeros of P_0 at exactly the line frequency of interest.

Since this is an important point, a graphical interpretation will now be presented. P_0 is zero whenever the impedance seen by P_I is the negative of $j\omega L_P$. Since the zeros of P_I in the frequency range of interest are given by (10), these are independent of L_I . The poles of P_I are either ω_L (if $L_I = 0$) or ω_S (if $L_I \neq 0$). Thus a plot of the impedance seen by P_I and a plot of $-j\omega L_P$ intersect at ω_0 , the zero of P_0 . Such a plot is shown in Figure 2. From this figure it can be seen that ω_0 can vary anywhere from ω_S up to a frequency ω_1 which satisfies equation (10). Hence, some optimal L_P yields $\omega_0 = \omega_L$.

Effect of Pulser Line Impedance on System Poles

If it is assumed that the pulser line is pressure fed through an impedance Z_D , it can be shown that the condition for system resonance becomes

$$\frac{1}{jZ_C} \frac{\frac{jZ_C}{Z_I} - \tan \omega l_1/a}{1 + j \frac{Z_C}{Z_I} \tan \omega l_1/a} + \frac{1}{jZ_C} \frac{jZ_C/Z_O - \tan \omega l_2/a}{1 + j \frac{Z_C}{Z_O} \tan \omega l_2/a} + \frac{1}{Z_D} = 0 \quad (26)$$

If we let $Z_I = j\omega L_I$, $Z_O = \frac{1}{j\omega C_B}$, $Z_D = j\omega L_D$, $\omega^2 = y$ and assume $\tan \omega l/a \approx \omega l/a$, then equation (26) becomes

$$C_B L_I Z_C \frac{l_1 l_2}{a^2} y^2 - y \left[\left(\frac{L_I}{a} + \frac{C_B Z_C^2}{a} \right) (l_1 + l_2) + L_I Z_C C_B \left(1 + \frac{Z_C l_2}{a L_D} \right) \right. \\ \left. + \frac{Z_C l_1 l_2}{a^2} \left(1 + \frac{C_B Z_C^2}{L_D} \right) \right] + Z_C \left(1 + \frac{L_I}{L_D} + \frac{Z_C l_1}{a L_D} \right) = 0 \quad (27)$$

For simplicity assume $L_I=0$. Then the solution of (27) is

$$\omega_{LD}^2 = \frac{(1 + Z_C l_1/a L_D)}{C_B Z_C \frac{(l_1 + l_2)}{a} + \frac{l_1 l_2}{a^2} \left(1 + \frac{C_B Z_C^2}{L_D} \right)} \quad (28)$$

where ω_{LD} is the resonance of the test facility with $L_I=0$ and $L_D \neq 0$. In practice $C_B Z_C^2 \ll L_D$. Furthermore the assumption $\tan \omega l/a \approx \omega l/a$ implies a large wave speed a . Since

$$\frac{Z_{C^{\ell}1}}{a} = \frac{\ell_1}{Ag}$$

is the inertance of that portion of the test line above the pulser, a good rule of thumb is that if L_D is an order of magnitude larger than the line inertance, the test facility and line frequency will agree. Stated another way: if L_D is large enough the pulser line does not shift the system resonances. (This is also obvious from (26).)

Conclusions of Theoretical Analysis

The portion of the test facility above the sump tends to lower the test facility resonance compared to the line resonance. The smaller the inertance of this portion of the test facility, the closer the facility resonance approaches that of the line. Since the addition of the accumulator reduces this inertance, the second test was better, in this respect, than the first.

If the line resonances are defined at the relative maximum of the ratio of pump pressure to pulser line pressure, and it is assumed that this occurs at the minimum of pulser line pressure, then the test facility could yield solutions which are anywhere from 10% too small to 20% too high, depending on the distance between the pulser pressure transducer and the line. For a fixed inertance above the sump, the resonance thus determined is higher the shorter this distance. No attempt was made to determine which of the two tests was theoretically better in this regard.

The location of the pulser line is immaterial. The impedance of the pulser line is high enough so that there is little shift in the resonance of the test facility due to the pulser.

The theoretical analysis presented does not explain why the PSD's of different pressure peak at different frequencies or why the pressure ratios show "glitches". However, the analysis assumes that the forcing signal is independent of frequency. Actually the pulser used in the test tends to reduce its output above ten hertz. The result of this would be to multiply the response curves of the pressure by that of the pulser. The relative maximum of the result then depends on the nature of the response near the maximum and it is quite likely that two different pressure responses could peak at the same frequency for a constant (with frequency) input but peak at different frequencies if the input is frequency dependent.

The tank can be represented by an inertance L_T as follows:

$$\lim_{\omega \rightarrow \infty} P_T = -j\omega \frac{h_T}{gA_T} \dot{W}_T = -j\omega L_T \dot{W}_T \quad (30)$$

where $L_T = \frac{h_T}{gA_T}$.

Lox Accumulator

The lox accumulator is modelled as a passive impedance Z_A .* If P_A , \dot{W}_A are the pressure and flow variations into the accumulator, then

$$P_A = Z_A \dot{W}_A \quad (31)$$

where

$$Z_A = j\omega L_A - j \frac{1}{\omega C_A}$$

$$L_A = \frac{1}{g} \int_0^{\ell_A} \frac{d\ell}{A(\ell)}$$

$$C_A = \frac{\rho V_{AO}}{\gamma P_{AO}}$$

ρ = weight density of fluid

*For a derivation of these equations see R. L. Goldman and G. C. Reis, "A Method for Determining the POGO Stability of Large Launch Vehicles", RIAS Technical Report, TR 69-7C; May 1969, section 2.1.

l_A = height of fluid in the accumulator

$A(l)$ = area versus height

P_{AO} , V_{AO} are static gas pressure and volume, resp.

γ = dimensionless isentropic exponent (≈ 1.66)

Lox Sump

For the present, the sump dynamics are neglected. Hence the pressure is uniform and continuity of flow is assumed. Thus if

P_{ST} , \dot{W}_{ST} are pressure, flow from tank line

P_{SL} , \dot{W}_{SL} are pressure, flow into suction line

P_{SA} , \dot{W}_{SA} are pressure, flow into accumulator line

then

$$P_{ST} = P_{SL} = P_{SA} = P_S \text{ sump pressure}$$

$$\dot{W}_{ST} = \dot{W}_{SL} + \dot{W}_{SA}$$

Lox Line Load (bubble, pump, discharge line)

Let P_p , \dot{W}_p be pressure and flow variations out of suction line. Then the pressure-flow variables into the pump (P_p , \dot{W}_{PI}) are defined by

$$\dot{W}_{PI} = \dot{W}_p - j\omega C_B P_p \quad (32)$$

where C_B = cavitation compliance. If P_{PO} , \dot{W}_{PO} are the downstream pump pressure and flow then

$$P_{PO} = K_p P_p - R_p \dot{W}_{PO} \quad (33)$$

where K_p = pump gain

R_p = pump resistance.

Assuming no pressure variations in the "bobtail engine", and approximating the pump discharge line as loss plus inertance yields

$$P_{PO} = K_P P_P - R_P \frac{P_{PO}}{R_D + j\omega L_D} \quad (34)$$

where R_D = discharge resistance

L_D = discharge inertance.

Letting $\dot{W}_{PI} = \dot{W}_{PO}$ and combining yields

$$\dot{W}_P - j\omega C_B P_P = W_{PI} = \frac{K_P P_P - P_{PO}}{R_P} = \frac{K_P}{R_P} P_P - \frac{1}{R_P} \frac{K_P}{1 + \frac{R_P}{R_D + j\omega L_D}} P_P \quad (35)$$

or

$$\begin{aligned} \dot{W}_P &= \left[\frac{K_P}{R_P} \left(1 - \frac{1}{1 + \frac{R_P}{R_D + j\omega L_D}} \right) + j\omega C_B \right] P_P \\ &= \left[j\omega C_B + \frac{K_P}{R_P + \frac{R_D + j\omega L_D}{K_P}} \right] P_P \end{aligned} \quad (36)$$

Hence the pump and discharge system can be represented by an impedance Z_P defined by

$$\frac{1}{Z_P} = j\omega C_B + \frac{1}{\frac{R_P + \frac{R_D + j\omega L_D}{K_P}}{K_P}} = Y_P \quad (37)$$

Test Facility Suction Lines

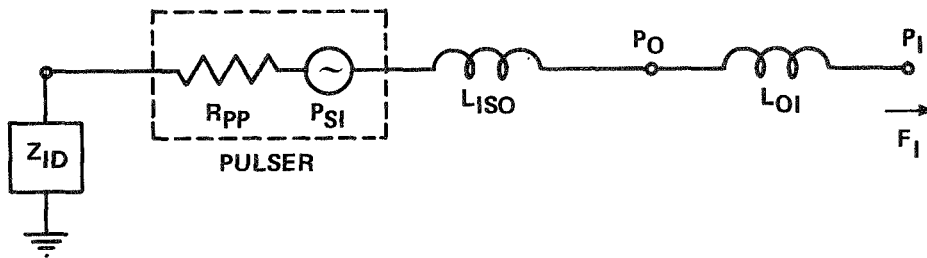
There are four major suction line segments in the test jig

- 1. between tank and sump Y_{TS}
- 2. between sump and pulser line Y_{SP}
- 3. between pulser line and pump Y_{PP}
- 4. between sump and accumulator Y_{SA}

Each line is to be represented as a 2×4 submatrix in the system of equations of the form $[Y I]$ where I is a 2×2 identity and Y is a 2×2 computed "back of the envelope" as the product of three matrices, thus $Y = -Y_1 Y_2 Y_3$, each Y_i being a segment of line represented as in equation 1. Hence, each of the four suction lines will be effectively modelled as three segments.

Pulser Line Equations

The pulser equations are linearized and the result modelled as a pressure source P_{SI} (which may be frequency dependent) and resistance R_{PP} . The rest of the pulser line is modelled as shown in the figure below. Here L_{OI} is the



Furthermore, the theoretical analysis assumes that the maximum of a ratio occurs at the minimum of the denominator which is not exactly true.

DERIVATION OF COMPUTER MODEL

Introduction

Although the theoretical analysis provides answers to the problems being considered, the use of simplifying assumptions need verification. In addition some aspects of the problem (e.g., pulser frequency response; the optimum placement of the pulser pressure transducer, etc.) are too complicated for "pencil and paper" calculations. Thus it was decided to construct a more complicated model of the test facility and subject it to computer analysis.

The model was designed to provide a steady-state sinusoidal analysis. Structural motion of the facility was neglected. Hence vertical and horizontal lines are indistinguishable. Furthermore, relative and absolute flows are equal. The fluid losses were neglected. We now proceed to derive the equations for each major portion of the test facility.

Lox Tank

It is assumed that the surface pressure of fluid in the tank is constant. If P_T is the pressure variation at the tank bottom, and \dot{W}_T is the flow variation out of the tank, then, by the results of Appendix A

$$P_T = -j \frac{\omega a_T}{g A_T} \left[\frac{1}{\omega} \tan \frac{\omega h_T}{a_T} \right] \dot{W}_T \quad (29)$$

where h_T is the height of fluid in the tank

a_T is the wave speed in the tank

A_T is the tank area.

inertance of the pulser line between the transducer (at P_0) and the junction of the pulser line and the line under test (at P_I). L_{ISO} is the inertance of the line between the pulser and the pulser pressure transducer. Z_{ID} is the impedance of the rest of the pulser line. Following the results of Appendix A, Z_{ID} can be written as

$$Z_{ID} = j \frac{a_p}{A_p g} \tan \frac{\omega \ell_{ID}}{a} \quad (38)$$

where ℓ_{ID} is the length of the pulser line between pulser and reservoir, and a_p , A_p are wave speed and area of pulser line.

The P_{SI} versus frequency information was taken from experimental data. If F_I is the flow out of the pulser line, then

$$F_I = \frac{P_{SI} - P_I}{Z_D} \quad (39)$$

where $Z_D = R_{PP} + Z_{ID} + j\omega(L_{ISO} + L_{OI})$.

The Computer Equations

Let \dot{W}_{I1} be the flow out of suction line 2 and \dot{W}_{I2} be the flow into suction line 3. Then

$$\dot{W}_{I1} + F_I = \dot{W}_{I2} \tag{40}$$

The system equations can now be written in matrix form as

		1	0	0	0	0	0	0	0	0	0	0	0	0	P_T	0
		0	0	0	0	0	0	1	0	0	0	0	0	0	\dot{W}_T	0
0	0	Y_{SP}		1	0	0	0	0	0	0	0	0	0	0	P_S	0
0	0			$\frac{1}{Z_D}$	1	0	0	0	0	0	0	0	0	0	\dot{W}_{SL}	$\frac{P_{PI}}{Z_D}$
0	0	0	0	Y_{PP}		0	0	0	0	0	1	0	0	0	P_I	0
0	0	0	0			0	0	0	0	0	0	1	0	0	\dot{W}_{I2}	0
0	0	Y_{SA}		0	0	0	Y_{SA}	0	1	0	0	0	0	0	\dot{W}_{SA}	0
0	0			0	0	0		0	0	1	0	0	0	0	\dot{W}_{ST}	0
0	0	0	-1	0	0	-1	1	0	0	0	0	0	0	0	P_A	0
0	0	0	0	0	0	0		1	$-Z_A$	0	0	0	0	0	\dot{W}_A	0
0	0	0	0	0	0	0	0	0	0	0	$-Y_P$	1	0	0	P_P	0
1	Z_T	0	0	0	0	0	0	0	0	0	0	0	0	0	\dot{W}_P	0

where each Y_{ij} is a 2 x 2 matrix found by multiplying three 2 x 2 matrices (e.g., $Y_{ij} = -Y_{ij1} Y_{ij2} Y_{ij3}$ with Y_{ijk} as in equation 1).

The computer solves this set of equations for each desired value of frequency ω , and thus provides the necessary response plots.

COMPUTER RESULTS *

Figures 3, 4 and 5 show the results of the computer analysis. These plots show resonant frequencies (as determined by maximum amplitude) as ordinate versus cavitation compliance C_{BO} as abscissa. In all these figures the heavy solid line is the resonant characteristics of the line and cavitation compliance only. (This is the quantity that the test is presumed to measure.) The light solid line is the ratio P_p/P_o , which is the quantity used in the test to determine the resonant frequency. The dotted lines show the relative maximum of the pump pressure P_p , and should therefore represent the test system resonances. The dashed lines show the resonances at the pulser transducer.

Figure 3 shows that the system resonance (as determined by P_p) is lowered about 10% by input inertance. Furthermore, P_o resonance is lower than system resonance, which verifies the theoretical prediction. In addition, the ratio of P_p/P_o is above the system resonance. It seems that the pulser transducer was placed fairly near the optimum location since the P_p/P_o ratio is close to the line characteristic.

Figure 4 shows that the P_p/P_o ratio is independent of pulser input, as expected. The slight shift in system resonance due to pulser variation is seen in the P_p plot. The fact that the pulser output decreases with frequency shifts the resonance of P_o drastically, as was expected. For emphasis, we repeat that the ratio of P_p/P_o still gives a good indication of the line characteristic.

As a measure of the effect of the load on the results, plots were made as for Figure 3, but with the downstream impedance removed. The results are shown in Figure 5.

*See A. T. Ackerman's Bellcomm Memo B69 10118 for further results.

CONCLUSIONS AND RECOMMENDATIONS

The computer analysis validates the conclusions of the theoretical analysis and shows that the test facility yields solutions for the line frequency which are fairly accurate. However, this happy fact seems to be due to a fortuitous set of circumstances. In order that future tests not rely so heavily on serendipity, the following recommendations are offered.

Since flow is the independent variable of the test, this should be measured. Then the difficulties which arise due to taking the ratio of dependent variables will not exist.

The accumulator resonance should be near the lower end of the expected frequency range of interest. This will reduce the input inertance during the test. Furthermore, the accumulator inertance should be as small as possible, consistent with the desired resonant frequency and gas compliance.

The pulser to be used in future tests should be flat over the frequency band of interest. The difficulties encountered in measuring a 25 hz. resonance with a pulser flat to only 10 hz. were made clear in this test. If such pulsers are not available, then some kind of theoretical analysis, suitable to the problem, should be performed so that "rules of thumb" (such as equation (25)) will yield a near optimum solution.

A frequency insensitive pulser would also allow for a better test in the following fashion. A tunable filter could extract the signal frequency from a pressure signal. Then the pulser frequency could be varied on-line to determine the maximum point, and, hence, the system resonance.

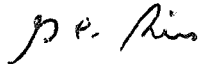
Further Applications of the Analysis

Shortly after the work described thus far had been completed, another occasion arose to use the computer program. Rocketdyne testing of the pumps indicated that the pump dynamics were much more significant than had been previously thought. They expressed concern that this new information would change the evaluation of the test results. By a suitable modification of the computer program, it was verified that the test results were still accurate, even with the new pump model.

At present, MSFC is conducting tests to determine the effect of adding accumulators to the second stage feed lines. Certain questions have developed and the program is again being modified to aid in analysis of these latest tests. Thus it seems that as long as this MSFC test facility is in operation the analysis reported here will be useful.

ACKNOWLEDGEMENTS

The author is grateful for discussions with R. V. Sperry and A. T. Ackerman. Without their critical comments, this memorandum could not have been written. The able programming assistance of C. B. Mummert is gratefully acknowledged. Thanks are due to L. D. Nelson for his careful review of this memo and for the many suggestions he made to improve it.



G. C. Reis

1033-GCR-jf

Attachments

Appendix A

Figures 1 - 5

BELLCOMM, INC.

APPENDIX A

In this appendix we derive an expression for the input impedance of a lossless line terminated in an impedance Z_0 . The matrix equation for the line of length ℓ is

$$\begin{bmatrix} P_1 \\ F_1 \end{bmatrix} = \begin{bmatrix} C & j Z_c S \\ j S/Z_c & C \end{bmatrix} \begin{bmatrix} P_2 \\ F_2 \end{bmatrix} \quad (A1)$$

where $C = \cos w \ell/a$ $S = \sin w \ell/a$

P_1 (P_2) is the inlet (outlet) pressure

F_1 (F_2) is the inlet (outlet) flow

Z_c is the characteristic impedance of the line.

The load impedance introduces the constraint

$$P_2 = Z_0 F_2 \quad (A2)$$

thus

$$\begin{bmatrix} P_1 \\ F_1 \end{bmatrix} = \begin{bmatrix} C & j Z_c S \\ j S/Z_c & C \end{bmatrix} \begin{bmatrix} Z_0 \\ 1 \end{bmatrix} F_2 \quad (A3)$$

The input impedance is thus given by

$$\frac{P_1}{F_1} = Z_c \frac{Z_0 C + j Z_c S}{Z_c C + j Z_0 S} \quad (A4)$$

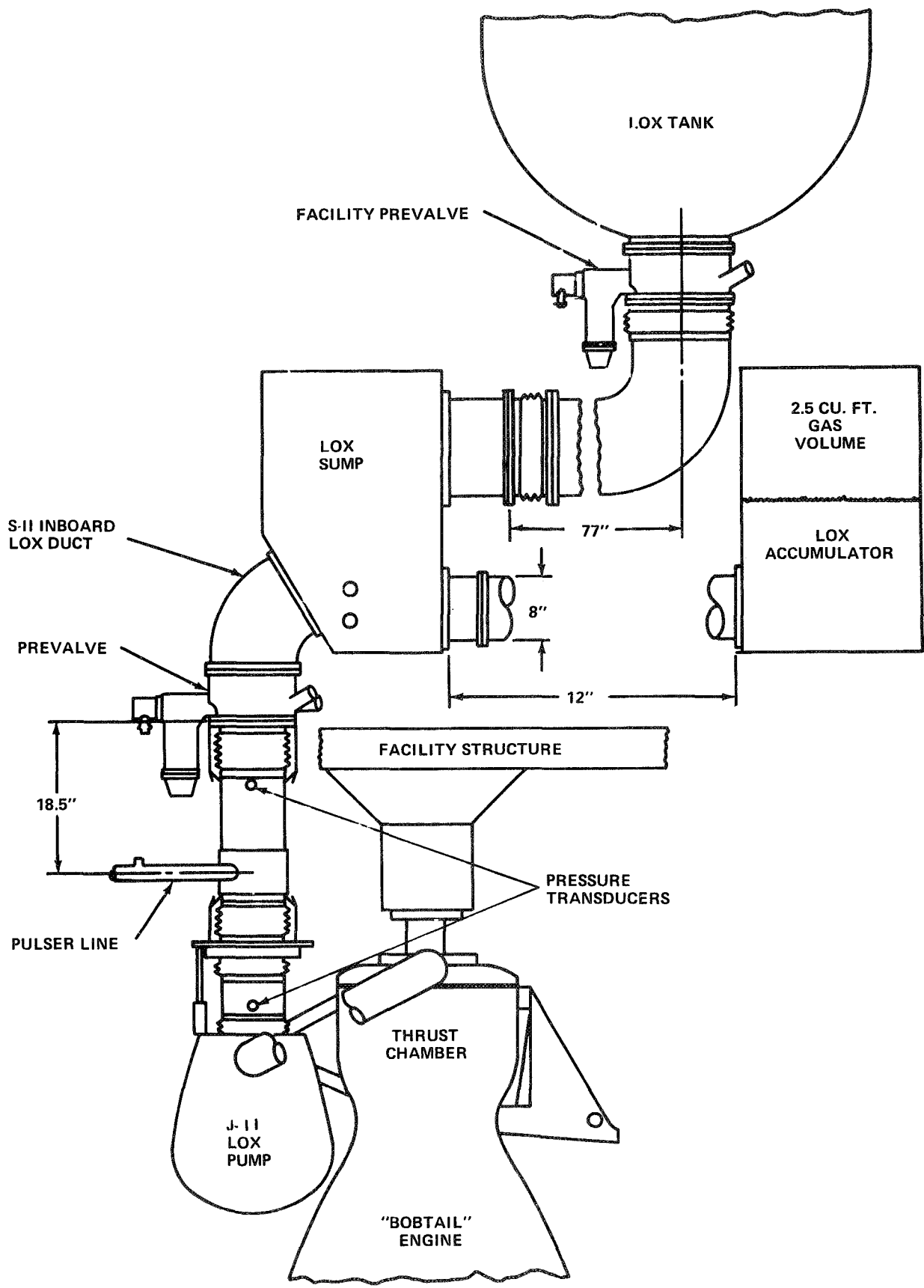
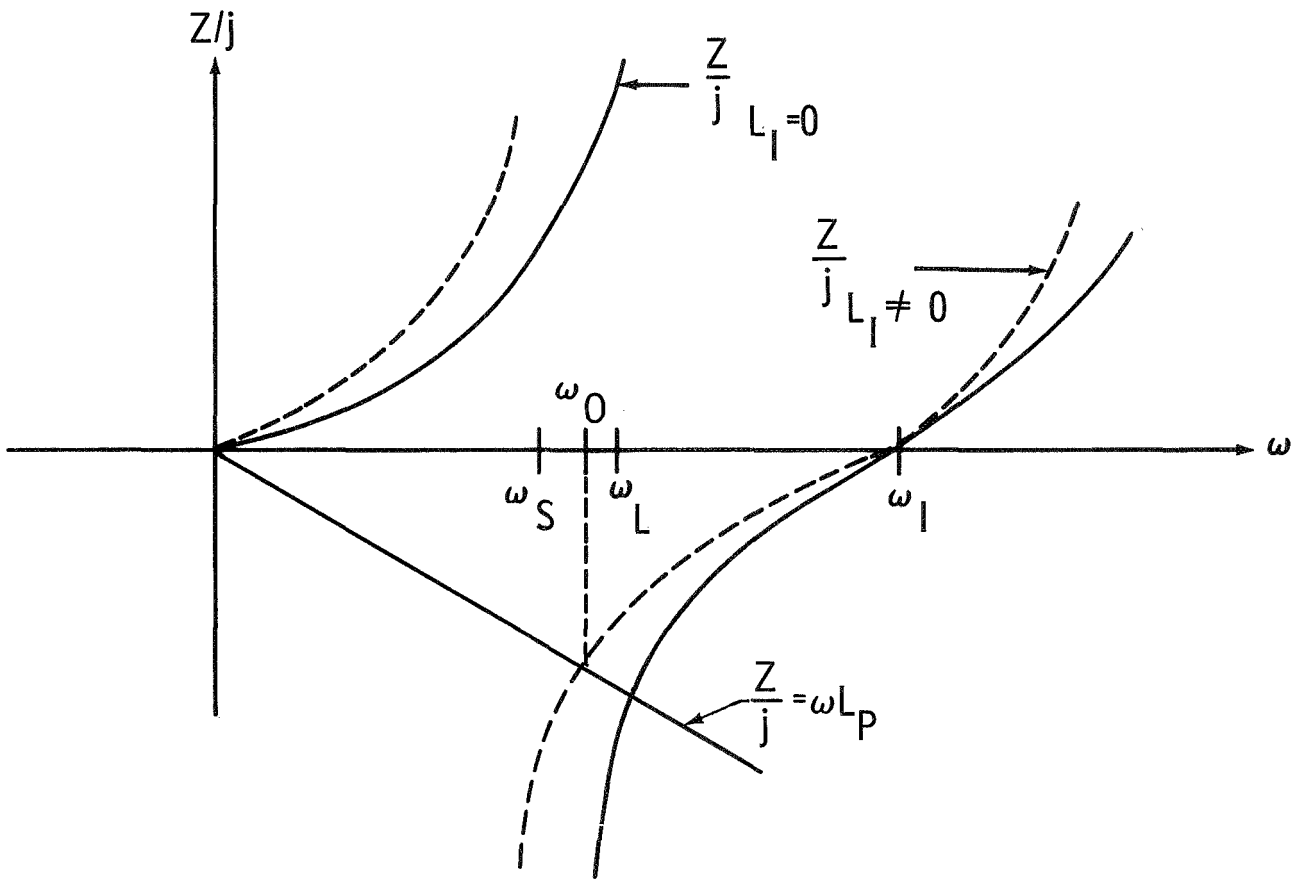


FIGURE 1



Z=IMPEDANCE SEEN BY P_I

FIGURE 2

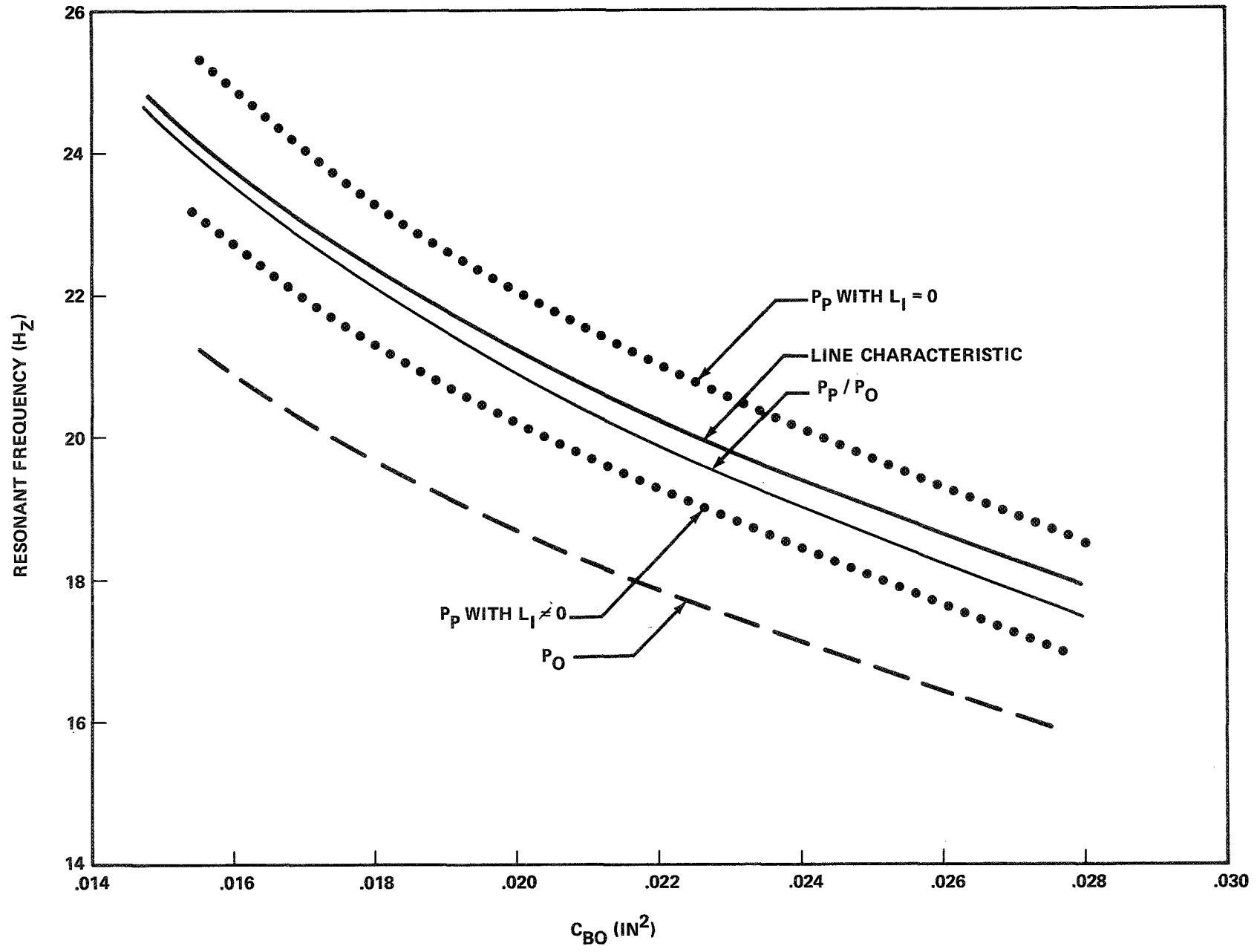


FIGURE 3- RESULTS FOR CONSTANT PULSER
LOADED LINE

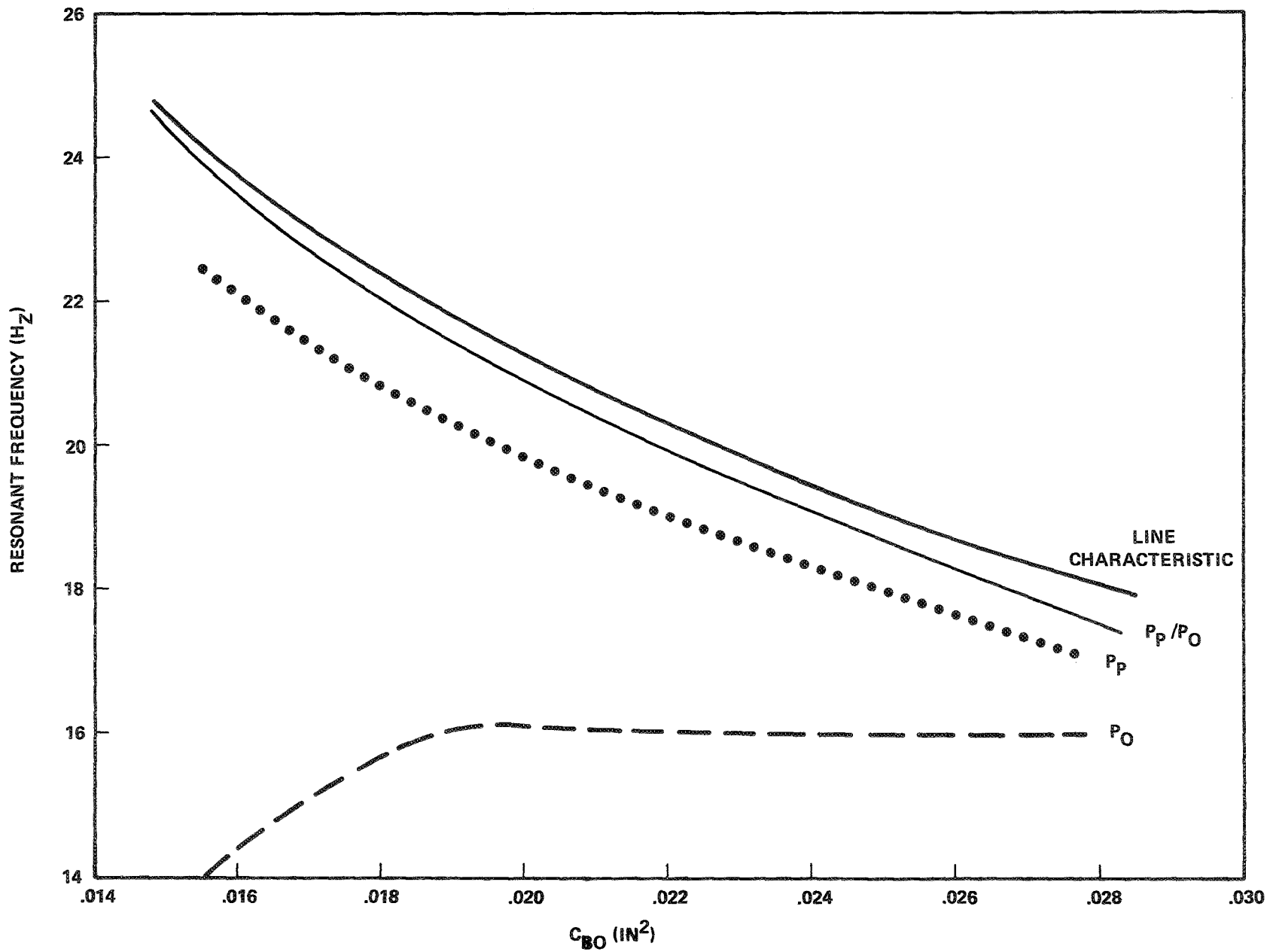


FIGURE 4- RESULTS FOR VARIABLE PULSER LOADED LINE

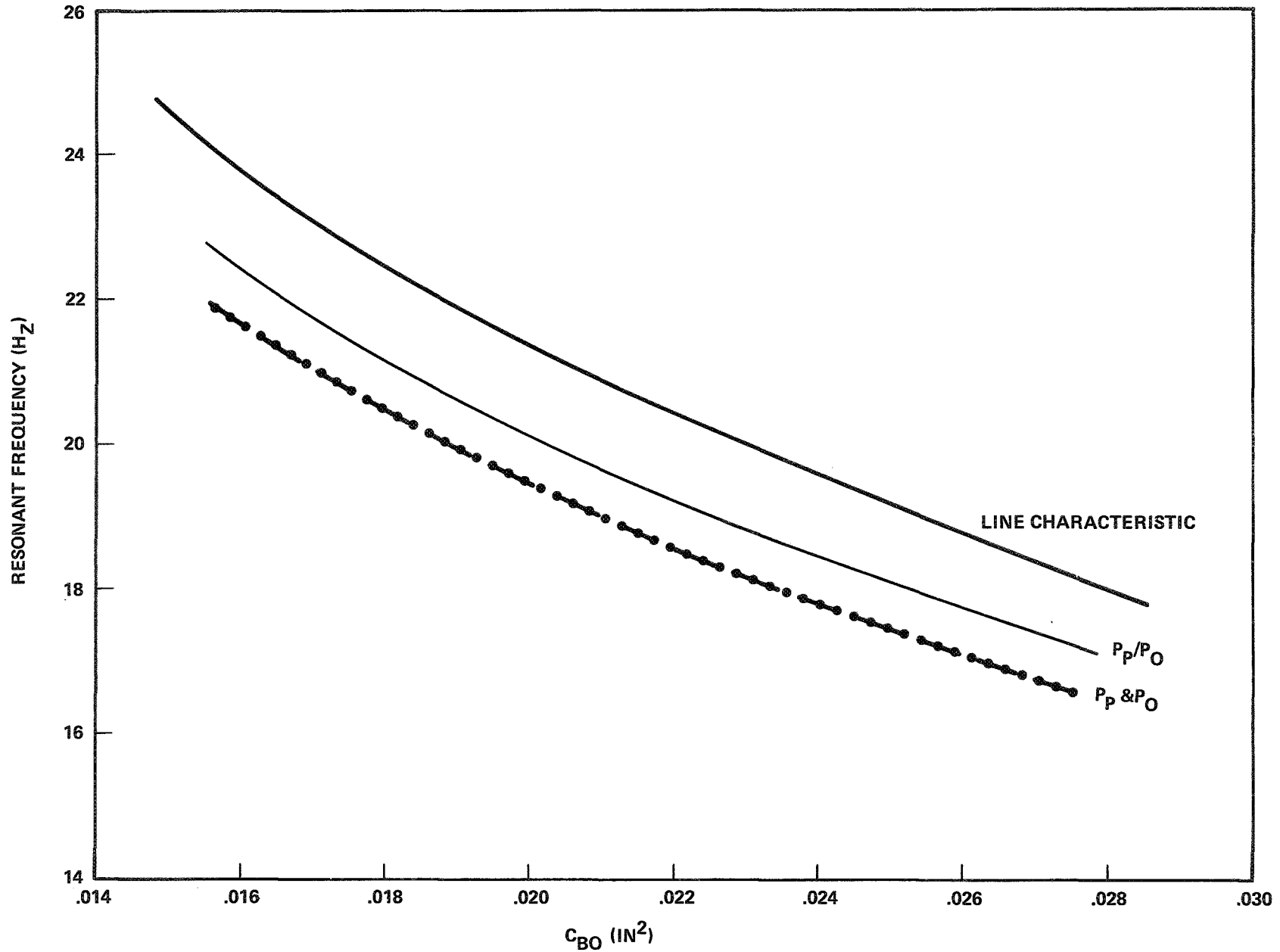


FIGURE 5- RESULTS FOR CONSTANT PULSER UNLOADED LINE